

Multi-Graph Transformer for Free-Hand Sketch Recognition

Peng Xu*, Chaitanya K. Joshi, and Xavier Bresson

Abstract—Learning meaningful representations of free-hand sketches remains a challenging task given the signal sparsity and the high-level abstraction of sketches. Existing techniques have focused on exploiting either the static nature of sketches with Convolutional Neural Networks (CNNs) or the temporal sequential property with Recurrent Neural Networks (RNNs). In this work, we propose a new representation of sketches as multiple sparsely connected graphs. We design a novel Graph Neural Network (GNN), the Multi-Graph Transformer (MGT), for learning representations of sketches from multiple graphs, which simultaneously capture global and local geometric stroke structures, as well as temporal information. We report extensive numerical experiments on a sketch recognition task to demonstrate the performance of the proposed approach. Particularly, MGT applied on 414k sketches from Google QuickDraw: (i) achieves small recognition gap to the CNN-based performance upper bound (72.80% vs. 74.22%) and infers faster than the CNN competitors, and (ii) outperforms all RNN-based models by a significant margin. To the best of our knowledge, this is the first work¹ proposing to represent sketches as graphs and apply GNNs for sketch recognition. Code and trained models are available at https://github.com/PengBoXiangShang/multigraph_transformer.

Index Terms—transformer, multi-graph transformer, MGT, graph neural network, GNN, sketch, free-hand sketch, hand-drawn sketch, sketch recognition, sketch classification, neural representation of sketch, graph representation of sketch.

I. INTRODUCTION

FREE-HAND sketches are drawings made without the use of any instruments. Sketches are different from traditional images: they are formed of temporal sequences of strokes [1], [2], while images are static collections of pixels with dense color and texture patterns. Sketches capture high-level abstraction of visual objects with very sparse information compared to regular images, which makes the modelling of sketches unique and challenging.

The modern prevalence of touchscreen devices has led to a flourishing of sketch-related applications in recent years, including sketch recognition [3], [4], sketch scene understanding [5], sketch hashing [2], sketch-based image retrieval [6], [7], [8], [9], [10], [11], sketch-related generation [1], [12], [13], [3], sketch self-supervised learning [14], [15], *etc.*

If we assume sketches to be 2D static images, CNNs can be directly applied to sketches, such as “Sketch-a-Net” [16]. If we now suppose that sketches are ordered sequences of point

Peng Xu, Chaitanya K. Joshi, and Xavier Bresson are with School of Computer Science and Engineering, Nanyang Technological University, Singapore.

* Corresponding to Peng Xu, email: peng.xu@ntu.edu.sg.

Xavier Bresson is supported in part by NRF Fellowship NRFF2017-10.

¹The preliminary version of this work can be found in arXiv <https://arxiv.org/abs/1912.11258v1> and <https://arxiv.org/abs/1912.11258v2>

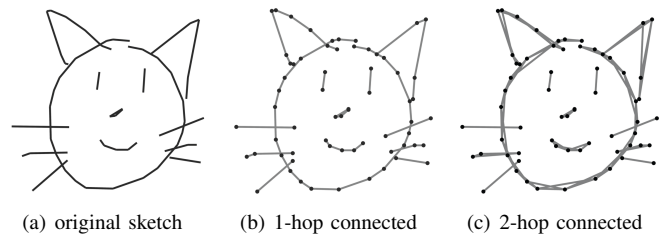


Fig. 1. Sketches can be seen as sets of curves and strokes, which are discretized by graphs.

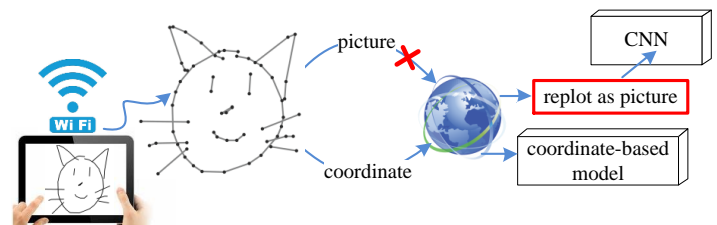


Fig. 2. In sketch-based human-computer interaction scenarios, it is time-consuming to render and transfer pictures of sketches. Solely transferring stroke coordinates leads to real-time applications.

coordinates, then RNNs can be used to recursively capture the temporal information, *e.g.*, “SketchRNN” [1].

In this work, we introduce a new representation of sketches with *graphs*. We assume that sketches are sets of curves and strokes, which are discretized by a set of points representing the graph nodes. This view offers high flexibility to encode different sketch geometric properties as we can decide different connectivity structures between the node points. We use two types of graphs to represent sketches: intra-stroke graphs and extra-stroke graphs. The first graphs capture the local geometry of strokes, independently to each other, with for example 1-hop or 2-hop connected graphs, see Figure 1. The second graphs encode the global geometry and temporal information of strokes. Another advantage of using graphs is the freedom to choose the node features. For sketches, spatial, temporal and semantic information is available with the stroke point coordinates, the ordering of points, and the pen state information, respectively. In summary, representing sketches with graphs offers a universal representation that can make use of global and local spatial sketch structures, as well as temporal and semantic information.

To exploit these graph structures, we propose a new Transformer [17] architecture that can use multiple sparsely connected graphs. It is worth reporting that a direct application of

the original Transformer model on the input spatio-temporal features provides poor results. We argue that the issue comes from the graph structure in the original Transformer which is a fully connected graph. Although fully-connected word graphs work impressively for Natural Language Processing, where the underlying word representations themselves contain rich information, such dense graph structures provide poor innate priors/inductive bias [18] for 2D sketch tasks. Transformers require sketch-specific design coming from geometric structures. This led us to naturally extend Transformers to multiple arbitrary graph structures. Moreover, graphs provide more robustness to handle noisy and style-changing sketches as they focus on the geometry of strokes and not on the specific distribution of points.

Another advantage of using domain-specific graphs is to leverage the sparsity property of discretized sketches. Observe that intra-stroke and extra-stroke graphs are *highly sparse* adjacency matrices. In practical sketch-based human-computer interaction scenarios, it is time-consuming to directly transfer the original sketch picture from user touch-screen devices to the back-end servers. To ensure real-time applications, transferring the stroke coordinates as a character string would be more beneficial, see Figure 2.

Our **main contributions** can be summarised as follows:

- 1) We propose to model sketches as sparsely connected graphs, which are flexible to encode local and global geometric sketch structures. To the best of our knowledge, it is the first time that graphs are proposed for representing sketches.
- 2) We introduce a novel Transformer architecture that can handle multiple arbitrary graphs. Using intra-stroke and extra-stroke graphs, the proposed *Multi-Graph Transformer* (MGT) learns both local and global patterns along sub-components of sketches.
- 3) Numerical experiments demonstrate the performances of our model. MGT significantly outperforms RNN-based models, and achieves small recognition gap to CNN-based architectures. Moreover, our MGT infers faster than the strongest CNN baseline (see details in Section IV-B7). This is promising for real-time sketch-based human-computer interaction systems. Note that for sketch recognition, CNNs are the performance upper bound of coordinate-based models that involve truncating coordinate sequences, *e.g.*, RNN or Transformer based architectures.
- 4) This Multi-Graph Transformer model is agnostic to graph domains, and can be used beyond sketch applications. We transfer our multi-graph transformer idea to conduct Relation Extraction on a NLP benchmark, *i.e.*, SemEval-2010 task 8, outperforming the state-of-the-art CNNs by a clear margin (prediction acc.: ours (89.45%) vs. CNN (86.60%)).

From the perspective of representing sketches and the practical sketch-oriented applications, the **main advantages** of our proposed Multi-Graph Transformer against CNN are:

- 1) Our model can be used for real-time sketch-based HCI (Human Computer Interaction) systems, because it

does not need to render and transfer sketch pictures (see Figure 2).

- 2) Our MGT is faster than the strongest CNN baseline, *i.e.*, Inception V3. This will be demonstrated by experiments in Section IV-B7.
- 3) As demonstrated in [19], coordinate-based models (*e.g.*, our MGT, RNNs) are more suitable than CNNs for the stroke-level tasks, *e.g.*, perceptual grouping, stroke-grained segmentation.
- 4) Our MGT takes the stroke sequence as input, thus it can handle the tasks that need to understand the logic and timing patterns of sketching process, *e.g.*, stroke-by-stroke generation, stroke-level abstraction. Specifically, stroke-by-stroke sketch generation needs models learn the temporal information, because the models need to decide the order of stroke generation. However, as discussed in [20], CNNs intrinsically fail to work for these tasks.

The rest of this paper is organized as follows: Section II briefly summarizes related work. Section III describes our proposed Multi-Graph Transformer. Experimental results and discussion are presented in Section IV, followed by a conclusion Section V. Finally, we discuss our future work in Section VI.

II. RELATED WORK

A. Neural Network Architectures for Sketches

CNNs are a common choice for feature extraction from sketches. “Sketch-a-Net” [16] is a representative CNN-based model having a sketch-specific architecture. It was directly inspired from AlexNet [21] with larger first layer filters, no layer normalization, larger pooling sizes, and high dropout. Song *et al.* [22] further improved Sketch-a-Net by adding spatial-semantic attention layers. “SketchRNN” [1] is a seminal work to model temporal stroke sequences with RNNs, by taking the key point coordinates of stroke as input. “SketchRNN” reminds the researchers that sketching is a dynamic process so that the temporal patterns of sketching strokes should also be considered.

Recently, some CNN-RNN hybrid architectures have been proposed for sketches, *e.g.*, dual-branch networks [23], [2], cascaded networks [4], [24]. For more detailed summary and comparison for sketch representing networks, please check a comprehensive survey [20].

Essentially, the aforementioned CNN or RNN -based network architectures model sketch in Euclidean space. How to model sketch in non-Euclidean spaces is an interesting question. In this work, we propose a novel Graph Neural Network architecture for learning sketch representations from multiple sparse graphs, combining both stroke geometry and temporal order.

B. Graph Neural Networks

Graph Neural Networks (GNNs) [25], [26], [27], [28], [29], [30], [31], [32] aim to generalize neural networks to non-Euclidean domains such as graphs and manifolds. GNNs

iteratively build representations of graphs through recursive neighborhood aggregation (or message passing), where each graph node gathers features from its neighbors to represent local graph structure. Recently, Graph Neural Networks have been widely applied for various domains, *e.g.*, vision, language. However, sketch-oriented Graph Neural Networks are still under-studied.

C. Transformers

The Transformer architecture [17], originally proposed as a powerful and scalable alternative to RNNs, has been widely adopted in the Natural Language Processing community for tasks such as machine translation [33], [34], language modelling [35], [36], and question-answering [37], [38].

Transformers for NLP can be regarded as GNNs which use self-attention [39], [40] for neighborhood aggregation on fully-connected word graphs [41]. However, GNNs and Transformers perform poorly when sketches are modelled as fully-connected graphs. This work advocates for the injection of inductive bias into Transformers through domain-specific graph structures.

III. METHOD

A. Notation

We assume that the training dataset D consists of N labeled sketches: $D = \{(\mathbf{X}_n, z_n)\}_{n=1}^N$. Each sketch \mathbf{X}_n has a class label z_n , and can be formulated as a S -step sequence $[\mathbf{C}_n, \mathbf{f}_n, \mathbf{p}] \in \mathbb{R}^{S \times 4}$. $\mathbf{C}_n = \{(x_n^s, y_n^s)\}_{s=1}^S \in \mathbb{R}^{S \times 2}$ is the coordinate sequence of the sketch points \mathbf{X}_n . All sketch point coordinates have been uniformly scaled to $x_n^s, y_n^s \in [0, 256]^2$. If the true length of \mathbf{C}_n is shorter than S then the vector $[-1, -1]$ is used for padding. Flag bit vector $\mathbf{f}_n \in \{f_1, f_2, f_3\}^{S \times 1}$ is a ternary integer vector that denotes the pen state sequence corresponding to each point of \mathbf{X}_n . It is defined as follows: f_1 if the point (x_n^s, y_n^s) is a starting or ongoing point of a stroke, f_2 if the point is the ending point of a stroke, and f_3 for a padding point. Vector $\mathbf{p} = [0, 1, 2, \dots, S-1]^T$ is a positional encoding vector that represents the temporal position of the points in each sketch \mathbf{X}_n .

Given D , we aim to model \mathbf{X}_n as multiple sparsely connected graphs and learn a deep embedding space, where the high-level semantic tasks can be conducted, *e.g.*, sketch recognition.

B. Multi-Modal Input Layer

Given a sketch \mathbf{X}_n , we model its S stroke points as S nodes of a graph. Each node has three features: (i) \mathbf{C}_n^s is the spatial positional information of the current stroke point s , (ii) \mathbf{f}_n^s is the pen state of the current stroke point. This information helps to identify the stroke points belonging to the same stroke, and (iii) \mathbf{p}^s is the temporal information of the current stroke point. As sketching is a dynamic process, it is important to use the temporal information.

The complete model architecture for our Multi-Graph Transformer is presented in Figure 3. Let us start by describing the

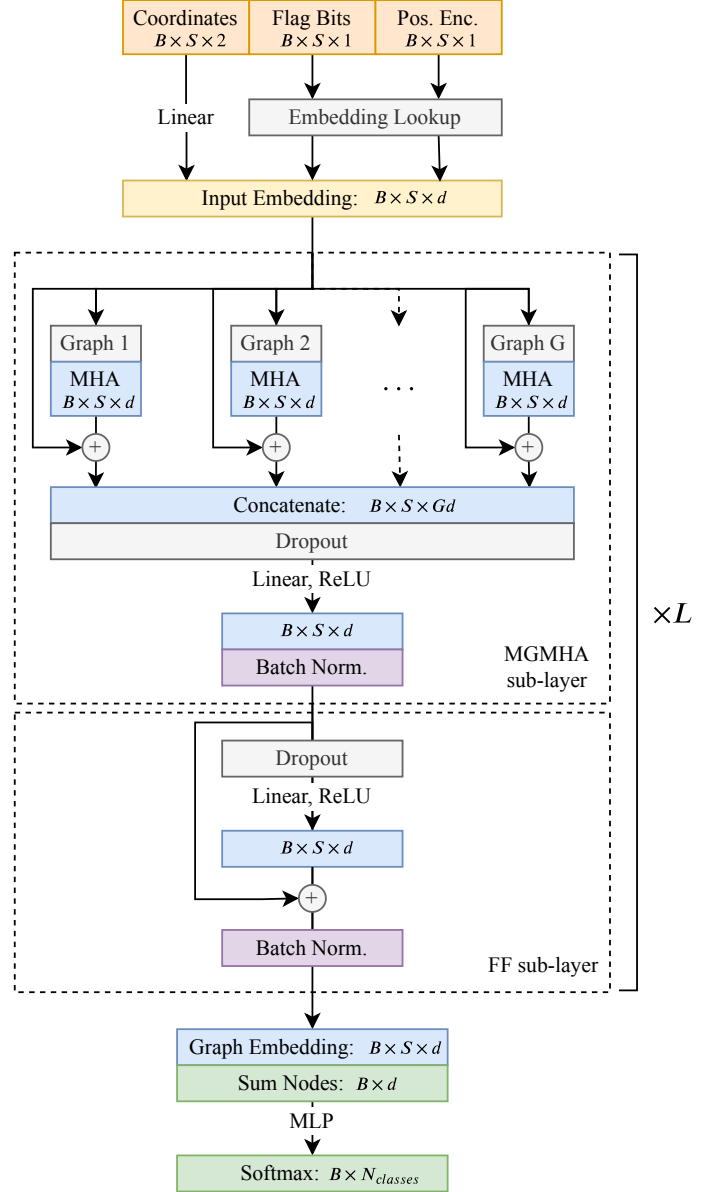


Fig. 3. Multi-Graph Transformer architecture. Each MGT layer is composed of (i) a Multi-Graph Multi-Head Attention (MGMHA) sub-layer and (ii) a position-wise fully connected Feed-Forward (FF) sub-layer. See details in text. “B” denotes batch size.

input layer. The final vector at node s of the multi-modal input layer is defined as

$$(\mathbf{h}_n^s)^{(l=0)} = \mathcal{C}(\mathcal{E}_1(\mathbf{C}_n^s), \mathcal{E}_2(\mathbf{f}_n^s), \mathcal{E}_2(\mathbf{p}^s)), \quad (1)$$

where $\mathcal{E}_1(\mathbf{C}_n^s)$ is the embedding of \mathbf{C}_n^s with a linear layer of size $2 \times d$, $\mathcal{E}_2(\mathbf{f}_n^s)$ and $\mathcal{E}_2(\mathbf{p}^s)$ are the embeddings of the flag bit \mathbf{f}_n^s (3 discrete values) and the position encoding \mathbf{p}^s (S discrete values) from an embedding dictionary of size $(S+3) \times d$, and $\mathcal{C}(\cdot, \cdot)$ is the concatenation operator. The node vector $(\mathbf{h}_n^s)^{(l=0)}$ has dimension $d = 3d$. The design of the input layer was selected after extensive ablation studies, which are described in subsequent sections.

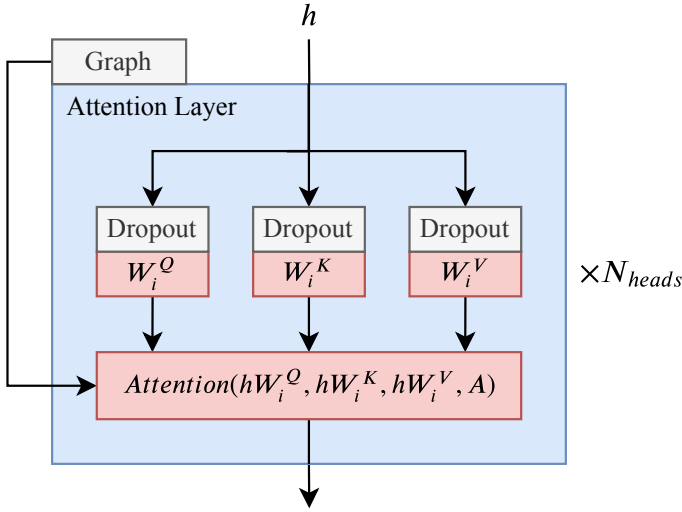


Fig. 4. Multi-Head Attention Layer, consisting of several Graph Attention Layers in parallel.

C. Multi-Graph Transformer

The initial node embedding $(\mathbf{h}_n^s)^{(l=0)}$ is updated by stacking L Multi-Graph Transformer (MGT) layers (7). Let us describe all layers.

1) *Graph Attention Layer*: Let \mathbf{A} be a graph adjacency matrix of size $S \times S$ and $\mathbf{Q} \in \mathbb{R}^{S \times d_q}$, $\mathbf{K} \in \mathbb{R}^{S \times d_k}$, $\mathbf{V} \in \mathbb{R}^{S \times d_v}$ be the query, key, and value matrices. We define a graph attention layer as

$$\text{GraphAttention}(\mathbf{Q}, \mathbf{K}, \mathbf{V}, \mathbf{A}) = \mathbf{A} \odot \text{softmax}\left(\frac{\mathbf{Q}\mathbf{K}^T}{\sqrt{d_k}}\right)\mathbf{V}, \quad (2)$$

where \odot is the Hadamard product. We simply weight the ‘‘Scaled Dot-Product Attention’’ [17] with the graph edge weights. We set $d_q = d_k = d_v = \frac{d}{I}$, where I is the number of attention heads.

2) *Multi-Head Attention Layer*: We aggregate the graph attentions with multiple heads:

$$\text{MultiHead}(\mathbf{Q}, \mathbf{K}, \mathbf{V}, \mathbf{A}) = \mathcal{C}(\text{head}_1, \dots, \text{head}_I)\mathbf{W}^O, \quad (3)$$

where $\mathbf{W}^O \in \mathbb{R}^{I d_v \times d}$ and each attention head is computed with the graph attention layer (2):

$$\text{head}_i = \text{GraphAttention}(\mathbf{Q}\mathbf{W}_i^Q, \mathbf{K}\mathbf{W}_i^K, \mathbf{V}\mathbf{W}_i^V, \mathbf{A}), \quad (4)$$

where $\mathbf{W}_i^Q \in \mathbb{R}^{d \times d_q}$, $\mathbf{W}_i^K \in \mathbb{R}^{d \times d_k}$, and $\mathbf{W}_i^V \in \mathbb{R}^{d \times d_v}$. We add dropout [42] before the linear projections of \mathbf{Q} , \mathbf{K} and \mathbf{V} . An illustration of the Multi-Head Attention Layer is presented in Figure 4.

3) *Multi-Graph Multi-Head Attention Layer*: Given a set of adjacency graph matrices $\{\mathbf{A}_g\}_{g=1}^G$, we can concatenate Multi-Head Attention Layers:

$$\text{MultiGraphMultiHeadAttention}(\mathbf{Q}, \mathbf{K}, \mathbf{V}, \{\mathbf{A}_g\}_{g=1}^G) = \text{ReLU}(\mathcal{C}(\text{ghead}_1, \dots, \text{ghead}_G)\mathbf{W}^{\tilde{O}}), \quad (5)$$

where $\mathbf{W}^{\tilde{O}} \in \mathbb{R}^{Gd \times d}$ and each Multi-Head Attention Layer is computed with (3):

$$\text{ghead}_g = \text{MultiHead}(\mathbf{Q}, \mathbf{K}, \mathbf{V}, \mathbf{A}_g). \quad (6)$$

4) *Multi-Graph Transformer Layer*: The Multi-Graph Transformer (MGT) at layer l for node s is defined as

$$\begin{aligned} (\mathbf{h}_n^s)^{(l)} &= \text{MGT}((\mathbf{h}_n^s)^{(l-1)}) \\ &= \hat{\mathbf{h}}_n^s + \text{FF}^{(l)}(\hat{\mathbf{h}}_n^s), \end{aligned} \quad (7)$$

where the intermediate feature representation $\hat{\mathbf{h}}_n^s$ is defined as:

$$\hat{\mathbf{h}}_n^s = (\text{MGMHA}_n^s)^{(l)}((\mathbf{h}_n^1)^{(l-1)}, \dots, (\mathbf{h}_n^S)^{(l-1)}). \quad (8)$$

The MGT layer is thus composed of (i) a Multi-Graph Multi-Head Attention (MGMHA) sub-layer (5) and (ii) a position-wise fully connected Feed-Forward (FF) sub-layer. Each MHA sub-layer (6) and FF (7) has residual-connection [43] and batch normalization [44]. See Figure 3 for an illustration.

D. Sketch Embedding and Classification Layer

Given a sketch \mathbf{X}_n with t_n key points, its continuous representation \mathbf{h}_n is simply given by the sum over all its node features from the last MGT layer:

$$\mathbf{h}_n = \sum_{s=1}^{t_n} (\mathbf{h}_n^s)^{(L)}. \quad (9)$$

Finally, we use a Multi-Layer Perceptron (MLP) to classify the sketch representation \mathbf{h}_n , see Figure 3.

E. Sketch-Specific Graphs

In this section, we discuss the graph structures we used in our Graph Transformer layers. We considered two types of graphs, which capture local and global geometric sketch structures.

The first class of graphs focus on representing the local geometry of individual strokes. We choose K -hop graphs to describe the local geometry of strokes. The intra-stroke adjacency matrix is defined as follows:

$$\mathbf{A}_{n,ij}^{K\text{-hop}} = \begin{cases} 1 & \text{if } j \in \mathcal{N}_i^{K\text{-hop}} \text{ and } j \in \text{global}(i), \\ 0 & \text{otherwise,} \end{cases} \quad (10)$$

where $\mathcal{N}_i^{K\text{-hop}}$ is the K -hop neighborhood of node i and $\text{global}(i)$ is the stroke of node i .

The second class of graphs capture the global and temporal relationships between the strokes composing the whole sketch. We define the extra-stroke adjacency matrix as follows:

$$\mathbf{A}_{n,ij}^{\text{global}} = \begin{cases} 1 & \text{if } |i - j| = 1 \text{ and } \text{global}(i) \neq \text{global}(j), \\ 0 & \text{otherwise.} \end{cases} \quad (11)$$

This graph will force the network to pay attention between two points belonging to two distinct strokes but consecutive in time, thus allowing the model to understand the relative arrangement of strokes.

TABLE I
SUMMARY STATISTICS FOR OUR SUBSET OF QUICKDRAW.

Set	# Samples	# Truncated (ratio)	# Key Points			
			max	min	mean	std
Training	345,000	11788 (3.42%)	100	2	43.26	21.85
Validation	34,500	1218 (3.53%)	100	2	43.24	21.89
Test	34,500	1235 (3.58%)	100	2	43.20	21.93

IV. EXPERIMENTS

A. Experimental Setting

In this section, we detail our experimental settings.

1) *Dataset and Pre-Processing:* Google QuickDraw [1]^{2 3} is the largest available sketch dataset containing 50 Million sketches as simplified stroke key points in temporal order, sampled using the Ramer–Douglas–Peucker algorithm after uniformly scaling image coordinates within 0 to 256. Unlike smaller crowd-sourced sketch datasets, *e.g.*, TU-Berlin [45], QuickDraw samples were collected via an international online game where users have only 20 seconds to sketch objects from 345 classes, such as cats, dogs, clocks, *etc.* Thus, sketch classification on QuickDraw not only involves a diversity of drawing styles, but can also be highly abstract and noisy, making it a challenging and practical test-bed for comparing the effectiveness of various neural network architectures. Following recent practices [11], [2], we create random training, validation and test sets from the full dataset by sampling 1000, 100 and 100 sketches respectively from each of the 345 categories in QuickDraw. Although the transformer architecture is able to handle sketches with any finite number of key points, following [2], we truncate or pad all samples to a uniform length of 100 key points/steps to facilitate efficient training of RNN and GNN-based models, to save parameters and training time. We provide summary statistics for our training, validation and test sets in Table I, and histograms visualizing the key points per sketch are shown in Figure 5.

2) *Evaluation Metrics:* Our evaluation metric for sketch recognition is “top K accuracy”, the proportion of samples whose true class is in the top K model predictions, for values $k = 1, 5, 10$. (Note that $\text{acc.}@k = 1.0$ means 100%)

3) *Implementation Details:* For fair comparison under similar hardware conditions, all experiments were implemented in PyTorch [46]⁴ and run on one Nvidia 1080Ti GPU. For Transformer models, we use the following hyperparameter values: $S = 100$, $L = 4$, $\hat{d} = 128$, $G = 3$ ($\mathbf{A}^{1\text{-hop}}$, $\mathbf{A}^{2\text{-hop}}$, $\mathbf{A}^{\text{global}}$), and $I = 8$ (per graph) for our Base model (and $\hat{d} = 256$ for our Large model). Our FF sub-layer is a d -dimensional linear layer ($d = 3\hat{d}$) followed by ReLU [47] and dropout. The MLP Classifier consists of two $4\hat{d}$ -dimensional linear layers with ReLU and dropout,

²<https://quickdraw.withgoogle.com/data>

³<https://github.com/googlecreativelab/quickdraw-dataset>

⁴<https://pytorch.org/>

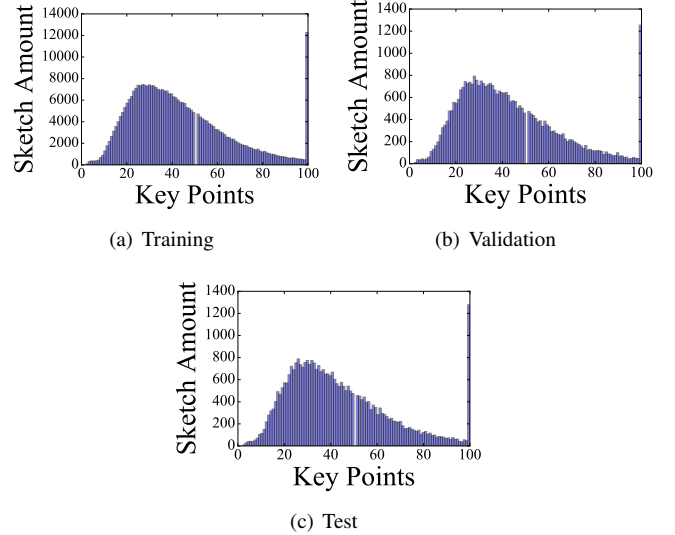


Fig. 5. Histograms of key points per sketch for our subset of QuickDraw. The sharp spike at 100 key points is due to truncation.

followed by a 345-dimensional linear projection representing logits over the 345 categories in QuickDraw. We train all models by minimizing the softmax cross-entropy loss using the Adam [48] optimizer for 100 epochs. We use an initial learning rate of $5e-5$ and multiply by a factor 0.7 every 10 epochs. We use an early stopping strategy (with the hyper-parameter “patience” of 10 epochs) for selecting the final model, and the checkpoint with the highest validation performance is chosen to report test performance.

4) *Baselines:* (i) From the perspective of coordinate-based sketch recognition, RNN models are a simple-yet-effective baseline. Following Xu *et al.* [2], we design several bi-directional LSTM [49] and GRU [50] models at increasing parameter budgets comparable with MGT. The final RNN states are concatenated and passed to the MLP classifier described previously. We use batch size 256, initial learning rate $1e-4$ and multiply by 0.9 every 10 epochs. We train models with both our multi-modal input (Section III-B) as well as the 4D input from [2].

(ii) Although converting sketch coordinates to images adds time overhead in practical settings and can be seen as auxiliary information, we compare MGT to various state-of-the-art CNN architectures. It is important to note that sketch sequences were truncated/padded for training both MGT and RNNs, hence image-based CNNs stand as an upper bound in terms of performance. For Inception V3 [51] and MobileNet V2 [52], initial learning rate is $1e-3$ and multiplied by 0.5 every 10 epochs. For other CNN baselines, the initial learning rate and decay are configured following their original papers. For each model, we use the maximum possible batch size. Following standard practice in computer vision [43], [53], we employ early stopping based on observing over-fitting in the validation loss, and select the checkpoint with the highest validation accuracy for evaluation on the test set.

(iii) To evaluate the effectiveness of the proposed Graph

Transformer layer, we compare it with popular GNN variants: the Graph Convolutional Network [29] and the Graph Attention Network [40]⁵. All GNN models follow the same hyper-parameter setup as Transformers ($L = 4$, $\hat{d} = 256$) and are augmented with residual connections and batch normalization for fair comparison, following [54]. Optimal hyper-parameters and learning rate schedules are selected based on validation set performance.

B. Results

For fair comparison with RNN and CNN baselines at various parameter budgets, we implement two configurations of MGT: Base (10M parameters) and Large (40M parameters). Additionally, we perform several ablation studies to evaluate the effectiveness of our multi-graph architecture and our sketch-specific input design. Our main results are presented in Table II.

1) *Comparison with RNN Baselines:* We trained RNNs at various parameter budgets, and present result for the best performing bi-directional LSTM and GRU models in Table II: (i) MGT outperforms both LSTM and GRU baselines by a significant margin (by 3% acc.@1 for Base, 5% for Large), indicating that both geometry and temporal order of strokes are important for sketch representation learning. (ii) Training larger RNNs is harder to converge, leading to degrading performance, *e.g.*, GRUs outperform deeper LSTMs by 2%.

These results are not surprising: RNNs are notoriously hard to train at scale [58], while Transformer performance is known to improve with scale, even with billions of model parameters [59].

2) *Comparison with CNN Baselines:* Table II also presents performance of several state-of-the-art CNN architectures for computer vision: (i) Inception V3 [51] and MobileNet V2 [52] are the best performing CNN architectures. Our MGT Base has competitive or better recognition accuracy than all other baselines: AlexNet [21], VGG-11 [55], ResNet models [43], and DenseNet-201 [53]. (ii) MGT Large has small performance gap to Inception V3 and MobileNet V2 (*i.e.*, 72.80% acc.@1 vs. 74.22%, 72.80% acc.@1 vs. 73.10%) and outperforms all other CNN architectures by almost 2%. (iii) Somewhat counter-intuitively, shallow networks (Inception V3, MobileNet V2) outperform deeper networks (ResNet-152, Densenet-201) by almost 2%. This result highlights that CNNs designed for images with dense colors and textures are un-suitable for sparse sketches.

Note that MobileNet V2 is specifically designed for fast inference on mobile phones and is not directly comparable in terms of model parameters.

3) *Ablations for Multi-Graph Architecture:* We design several ablation studies to evaluate our sketch-specific multi-graph architecture in Table III: (i) We evaluate Graph Transformers trained on fully-connected graphs, *i.e.* *vanilla* Transformers

(GT #1), fully-connected graphs within strokes (GT #2), as well as random graphs with 10%, 20% and 30% connectivity (GT #3, #4, and #5 respectively). We compare their performance with Graph Transformers trained on sketch-specific graphs $\mathbf{A}^{1\text{-hop}}$ (GT #6), $\mathbf{A}^{2\text{-hop}}$ (GT #7), $\mathbf{A}^{3\text{-hop}}$ (GT #8), and $\mathbf{A}^{\text{global}}$ (GT #9). We find that *vanilla* Transformers on fully-connected (52.49% acc.@1) and random graphs (52.71%, 53.52%, 53.22%) perform poorly compared to sketch-specific graph structures determined by domain expertise, such as fully-connected stroke graphs (64.87%) and $\mathbf{A}^{1\text{-hop}}$ (70.23%). The superior performance of K -hop graphs suggests that Transformers benefit from sparse graphs representing local sketch geometry. We also evaluate a combined sketch-specific graph structure, *i.e.*, $\mathbf{A}^{1\text{-hop}} \parallel \mathbf{A}^{2\text{-hop}} \parallel \mathbf{A}^{\text{global}}$ (GT #10), where the graph connectivity is the logical union set of $\mathbf{A}^{1\text{-hop}}$, $\mathbf{A}^{2\text{-hop}}$, and $\mathbf{A}^{\text{global}}$. However, this structure fails to gain performance improvement over $\mathbf{A}^{1\text{-hop}}$, $\mathbf{A}^{2\text{-hop}}$, and $\mathbf{A}^{\text{global}}$, despite involving more domain knowledge.

(ii) We experiment with various permutations of graphs for multi-graph models (MGT #11-#17). We find that using a 3-graph architecture (MGT #17) combining local sketch geometry ($\mathbf{A}^{1\text{-hop}}$, $\mathbf{A}^{2\text{-hop}}$) and global temporal relationships ($\mathbf{A}^{\text{global}}$) significantly boosts performance over 2-graph and 1-graph models (72.80% vs. 72.37% for 2-graph and 70.82% for 1-graph). This result is interesting because using global graphs independently (GT #9) leads to comparatively poor performance (54.88%). Additionally, we found that using diverse graphs (MGT #15, #17) is better than using the same graph (MGT #14). Comparing MGT #14 and MGT #6 further shows that performance gains are due to the multi-graph architecture as opposed to more model parameters.

(iii) We also repeatedly input the adjacency matrix of GT #10 (*i.e.*, $\mathbf{A}^{1\text{-hop}} \parallel \mathbf{A}^{2\text{-hop}} \parallel \mathbf{A}^{\text{global}}$) three times as the multiple graph structures to train our MGT (see MGT #16 in Table III). Compared with MGT #17, there is a clear performance gap (71.26% vs. 72.80%). This further validates our idea of learning sketch representations through multiple separate graphs.

4) *Comparison with GNN Baselines:* In Table IV, we present performance of our Graph Transformer model compared to Graph Convolutional Networks (GCN) [29] and Graph Attention Networks (GAT) [40], two popular GNN variants: (i) We find that all models perform similarly on fully-connected graphs. Using 1-hop graphs results in significant gains for all models, with Transformer performing the best. (ii) Interestingly, both GNNs on fully-connected graphs are outperformed by a simple position-wise embedding method without any graph structure: each node undergoes 4 feed-forward (FF) layers followed by summation and the MLP classifier. These results further highlights the importance of sketch-specific graph structures for the success of Transformers. Our final models use the Transformer layer, which implicitly includes the FF sub-layer (7).

5) *Ablations for Multi-Modal Input:* In Table V, we experiment with various permutations of our sketch-specific multi-modal input design. We aggregate information from

⁵For GAT, we use the same scaled dot-product attention mechanism as GT for efficiency.

TABLE II
TEST SET PERFORMANCE OF MGT VS. THE STATE-OF-THE-ART RNN AND CNN ARCHITECTURES. THE 1st/2nd/3rd BEST RESULTS PER COLUMN ARE INDICATED IN RED/BLUE/MAGENTA.

Network	Configurations	Recognition Accuracy			Parameter Amount
		acc.@1	acc.@5	acc.@10	
Bi-directional LSTM #1	4D Input, $\hat{d} = 256, L = 4, Dropout_{LSTM} = 0.5, Dropout_{MLP} = 0.15$	0.6665	0.8820	0.9189	5,553,241
Bi-directional LSTM #2	4D Input, $\hat{d} = 256, L = 5, Dropout_{LSTM} = 0.5, Dropout_{MLP} = 0.15$	0.6524	0.8697	0.9133	7,130,201
Bi-directional GRU	4D Input, $\hat{d} = 256, L = 5, Dropout_{GRU} = 0.5, Dropout_{MLP} = 0.15$	0.6768	0.8854	0.9234	5,419,097
AlexNet [21]	Standard architecture and configurations	0.6808	0.8847	0.9203	58,417,305
VGG-11 [55]		0.6743	0.8814	0.9191	130,179,801
Inception V3 [51]		0.7422	0.9189	0.9437	25,315,474
ResNet-18 [43]		0.7031	0.9030	0.9351	11,353,497
ResNet-34 [43]		0.7009	0.9010	0.9347	21,461,657
ResNet-152 [43]		0.6924	0.8973	0.9312	58,850,713
DenseNet-201 [53]		0.7050	0.9013	0.9331	18,755,673
MobileNet V2 [52]		0.7310	0.9161	0.9429	2,665,817
SCNet [56]		0.7123	0.9026	0.9351	24,222,489
ResNet-102+BSConv-U [57]		0.7172	0.9037	0.9334	7,029,791
Vanilla Transformer [17]	$\hat{d} = 256, L = 4, I = 8, Dropout = 0.1$, Fully-connected graph	0.5249	0.7802	0.8486	14,029,401
MGT (Base)	$\hat{d} = 128, L = 4, I = 24, Dropout = 0.1, \mathbf{A}^{1-hop}, \mathbf{A}^{2-hop}, \mathbf{A}^{global}$ graphs	0.7070	0.9030	0.9351	10,096,601
MGT (Large)	$\hat{d} = 256, L = 4, I = 24, Dropout = 0.25, \mathbf{A}^{1-hop}, \mathbf{A}^{2-hop}, \mathbf{A}^{global}$ graphs	0.7280	0.9106	0.9387	39,984,729

TABLE III
ABLATION STUDY FOR MULTI-GRAPH ARCHITECTURE OF MGT. GT DENOTES SINGLE-GRAPH VARIANTS OF MGT. THE 1st/2nd BEST RESULTS PER COLUMN ARE INDICATED IN RED/BLUE. || DENOTES THE LOGICAL UNION OPERATION.

Network	Configurations						Recognition Accuracy			Parameter Amount
	G	Graph Structure	I_{total}	\hat{d}	L	Dropout	acc.@1	acc.@5	acc.@10	
GT #1	1	Fully-connected (<i>vanilla</i>)	8	256	4	0.10	0.5249	0.7802	0.8486	14,029,401
GT #2	1	Intra-stroke Fully-connected	8	256	4	0.10	0.6487	0.8697	0.9151	14,029,401
GT #3	1	Random (10%)	8	256	4	0.10	0.5271	0.7890	0.8589	14,029,401
GT #4	1	Random (20%)	8	256	4	0.10	0.5352	0.7945	0.8617	14,029,401
GT #5	1	Random (30%)	8	256	4	0.10	0.5322	0.7917	0.8588	14,029,401
GT #6	1	\mathbf{A}^{1-hop}	8	256	4	0.10	0.7023	0.8974	0.9303	14,029,401
GT #7	1	\mathbf{A}^{2-hop}	8	256	4	0.10	0.7082	0.8999	0.9336	14,029,401
GT #8	1	\mathbf{A}^{3-hop}	8	256	4	0.10	0.7028	0.8991	0.9327	14,029,401
GT #9	1	\mathbf{A}^{global}	8	256	4	0.10	0.5488	0.8009	0.8659	14,029,401
GT #10	1	$\mathbf{A}^{1-hop} \mathbf{A}^{2-hop} \mathbf{A}^{global}$	8	256	4	0.10	0.7057	0.9021	0.9346	14,029,401
MGT #11	2	$\mathbf{A}^{1-hop}, \mathbf{A}^{2-hop}$	16	256	4	0.25	0.7149	0.9049	0.9361	28,188,249
MGT #12	2	$\mathbf{A}^{1-hop}, \mathbf{A}^{global}$	16	256	4	0.25	0.7111	0.9041	0.9355	28,188,249
MGT #13	2	$\mathbf{A}^{2-hop}, \mathbf{A}^{global}$	16	256	4	0.25	0.7237	0.9102	0.9400	28,188,249
MGT #14	3	$\mathbf{A}^{1-hop}, \mathbf{A}^{1-hop}, \mathbf{A}^{1-hop}$	24	256	4	0.25	0.7077	0.9020	0.9340	39,984,729
MGT #15	3	$\mathbf{A}^{1-hop}, \mathbf{A}^{2-hop}, \mathbf{A}^{3-hop}$	24	256	4	0.25	0.7156	0.9066	0.9365	39,984,729
MGT #16	3	$\mathbf{A}^{1-hop} \mathbf{A}^{2-hop} \mathbf{A}^{global}$	24	256	4	0.25	0.7126	0.9051	0.9372	39,984,729
MGT #17	3	$\mathbf{A}^{1-hop}, \mathbf{A}^{2-hop}, \mathbf{A}^{global}$	24	256	4	0.25	0.7280	0.9106	0.9387	39,984,729

TABLE IV
TEST SET PERFORMANCE OF GRAPH TRANSFORMER VS. OTHER GNN VARIANTS. THE 1st/2nd BEST RESULTS PER COLUMN ARE INDICATED IN RED/BLUE.

Network	Graph Structure	Recognition Accuracy			Parameter Amount
		acc.@1	acc.@5	acc.@10	
Graph Convolutional Networks (GCN) [29]	fully-connected	0.4098	0.7384	0.8213	6,948,441
	\mathbf{A}^{1-hop}	0.6800	0.8869	0.9224	
Graph Attention Networks (GAT) [40]	fully-connected	0.4098	0.6960	0.7897	11,660,889
	\mathbf{A}^{1-hop}	0.6977	0.8952	0.9298	
Graph Transformer (GT)	fully-connected	0.5242	0.7796	0.8465	14,029,401
	\mathbf{A}^{1-hop}	0.7057	0.8992	0.9311	
position-wise feed-forward	None	0.5296	0.7901	0.8576	4,586,073

TABLE V
ABLATION STUDY FOR MULTI-MODAL INPUT FOR MGT (LARGE). NOTATIONS: “+” AND “ $\mathcal{C}(\dots)$ ” DENOTE “SUM” AND “CONCATENATE”,
RESPECTIVELY. THE 1st/2nd BEST RESULTS PER COLUMN ARE INDICATED IN RED/BLUE.

Input Permutation	Recognition Accuracy		
	acc.@1	acc.@5	acc.@10
coordinate	0.6512	0.8735	0.9162
coordinate + flag bit	0.6568	0.8762	0.9176
coordinate + flag bit + position encoding	0.6600	0.8766	0.9182
\mathcal{C} (coordinate, flag bit)	0.7017	0.8996	0.9321
\mathcal{C} (coordinate, flag bit, position encoding)	0.7280	0.9106	0.9387
4D Input	0.6559	0.8758	0.9175
4D Input + position encoding	0.6606	0.8781	0.9190
\mathcal{C} (4D Input, position encoding)	0.7117	0.9048	0.9366

spatial (coordinates), semantic (flag bits), and temporal (position encodings) modalities via summation (as in Transformers for NLP) or concatenation: (i) Effectively using all modalities is important for performance (*e.g.*, “ \mathcal{C} (coordinate, flag bit, position encoding)” outperforms “coordinate” and “ \mathcal{C} (coordinate, flag bit)”: 72.80% acc.@1 vs. 65.12%, 70.17%). (ii) Concatenation works better than 4D input as well as summation (*e.g.*, “ \mathcal{C} (coordinate, flag bit, position encoding)” outperforms “ \mathcal{C} (4D Input, position encoding)” and “coordinate + flag bit + position encoding”: 72.80% vs. 71.17%, 66.06%).

6) *Qualitative Results*: In Figure 6 and Figure 7, we visualize attention heads at each layer of MGT for various test set samples. Each sub-figure contains attention heads for each of the three graphs ($\mathbf{A}^{1\text{-hop}}$, $\mathbf{A}^{2\text{-hop}}$, $\mathbf{A}^{\text{global}}$), and each of the rows #1-#4 in each sub-figure correspond to layers #1-#4. Darker reds indicate higher attention values. All figures are best viewed in color.

Attention heads in the initial layers attend very strongly to certain neighbors and very weakly to others, *i.e.*, the model builds local patterns for sketch sub-components (strokes) through message passing along their contours. In penultimate layers, the intensity of neighborhood attention is significantly lower and evenly distributed, indicating that the model is aggregating information from various strokes at each node.

Additionally, we believe $\mathbf{A}^{\text{global}}$ graphs are critical for message passing between strokes, enabling the model to understand their relative arrangement. For example, in Figure 6, both the head and feet of the bird are attached to the bottom of its body. In Figure 7, the feet of the teddy bear are associated.

7) *Comparison for Time Cost*: To demonstrate the speed advantage of our model, we also compare our MGT with the strongest CNN baselines, *i.e.*, Inception V3, MobileNet V2. We report the total time taken by models to perform inference over 34,500 sketches from the test set in Table VI. All models were implemented in PyTorch and run on an Intel Xeon CPU E5-2690 v4 server using a single Nvidia 1080Ti GPU, with batch size of 256 and 16 workers per run.

In Table VI, we observe: our MGT infers obviously faster

TABLE VI
EVALUATION TIMING COMPARISON FOR MULTI-GRAPH TRANSFORMER AND CNNs, AVERAGED OVER 3 RUNS. INFERENCE TIME IS THE TOTAL WALL CLOCK TIME FOR PERFORMING INFERENCE OVER 34,500 SKETCHES FROM THE TEST SET.

Network	Inference Time	Parameter Amount
Inception V3	2.682±0.154s	25,315,474
MobileNet V2	1.423±0.070s	2,665,817
MGT (Base)	0.849±0.044s	10,096,601
MGT (Large)	0.843±0.048s	39,984,729

TABLE VII
PERFORMANCE COMPARISON ON THE RELATION EXTRACTION TASK ON SEMEVAL-2010 TASK 8. THE 1st/2nd BEST RESULTS PER COLUMN ARE INDICATED IN RED/BLUE.

Network	Graph Structure	Prediction Accuracy
textual CNN [60]	-	0.8660
Transformer [61]	fully-connected	0.8900
Transformer	fully- and partially-connected	0.8945

than both Inception V3 and MobileNet V2.

Note that, unlike CNNs and RNNs, GNNs and GTs for sparse graph data formats are not natively supported by PyTorch. We believe that our MGT can infer faster in our future work, if we further speed up MGT via using the tailor-made GNN libraries such as Deep Graph Library⁶ and PyTorch Geometric⁷.

8) *Evaluation on Relation Extraction*: The main idea of our multi-graph transformer is injecting domain knowledge into Transformers through domain-specific graphs. We also try to evaluate this idea in other modalities beyond sketch, *e.g.*, NLP tasks. Thus, we transfer our multi-graph transformer idea to conduct Relation Extraction (RE) on a RE benchmark (SemEval-2010 task 8 [62]), outperforming the state-of-the-art CNNs by a clear margin (as reported in Table VII, prediction

⁶<https://www.dgl.ai/>

⁷https://github.com/rusty1s/pytorch_geometric

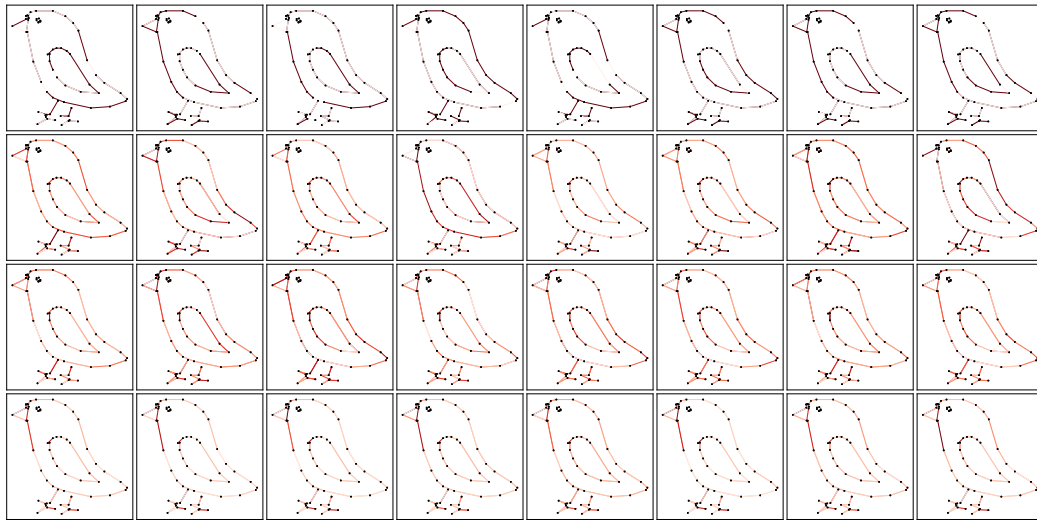
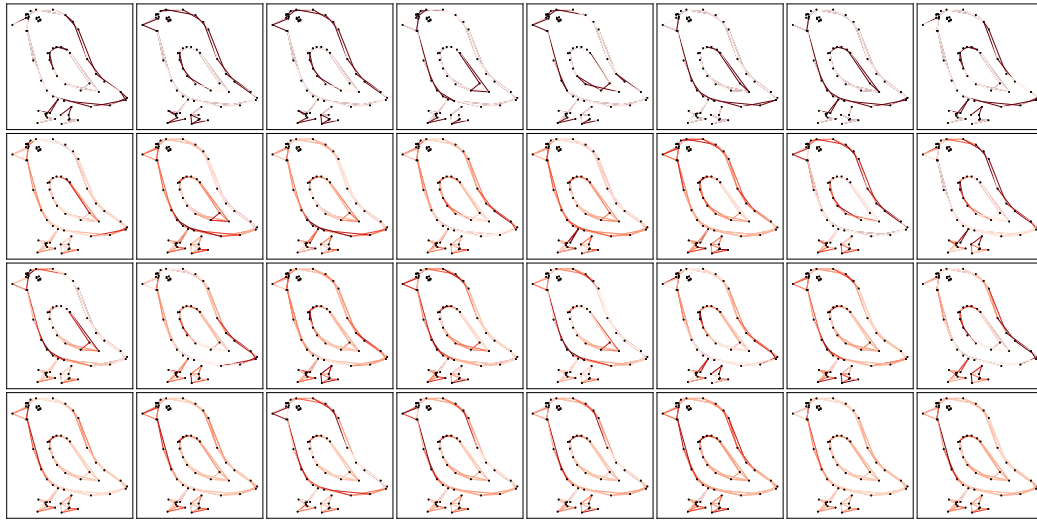
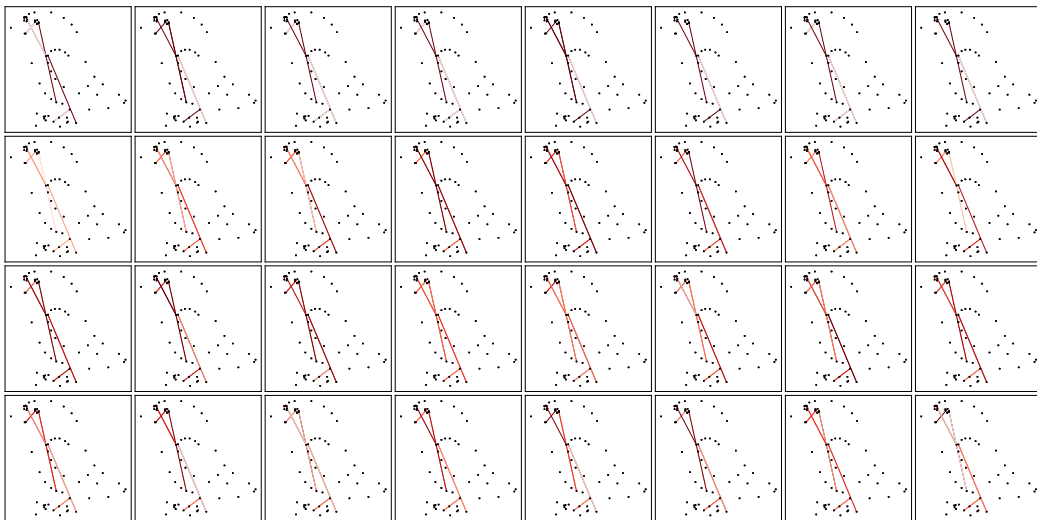
(a) $\mathbf{A}^{1\text{-hop}}$ (b) $\mathbf{A}^{2\text{-hop}}$ (c) $\mathbf{A}^{\text{global}}$

Fig. 6. Attention heads at each layer of MGT for a test set sample labelled *bird*. Each layer has $I = 8$ attention heads per graph in total. Darker reds indicate higher attention values. Best viewed in color.

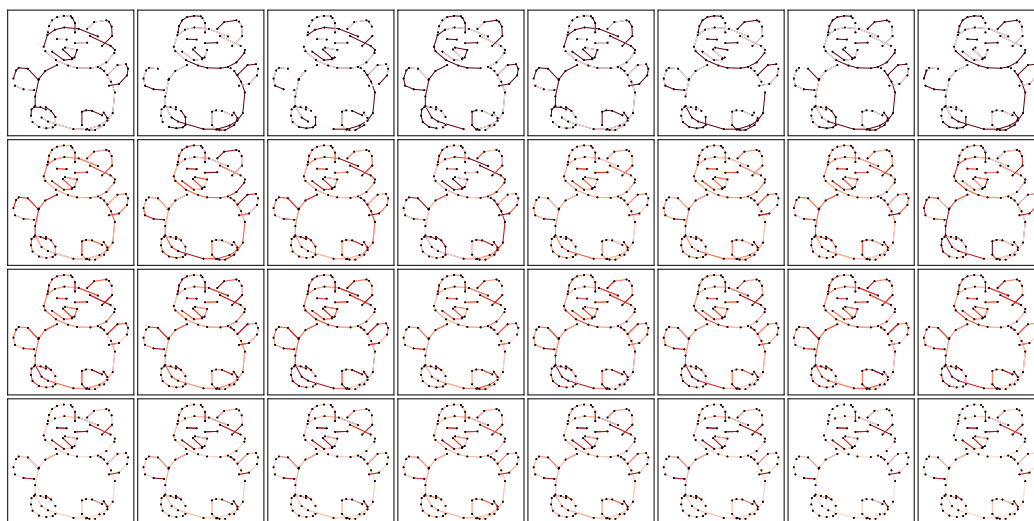
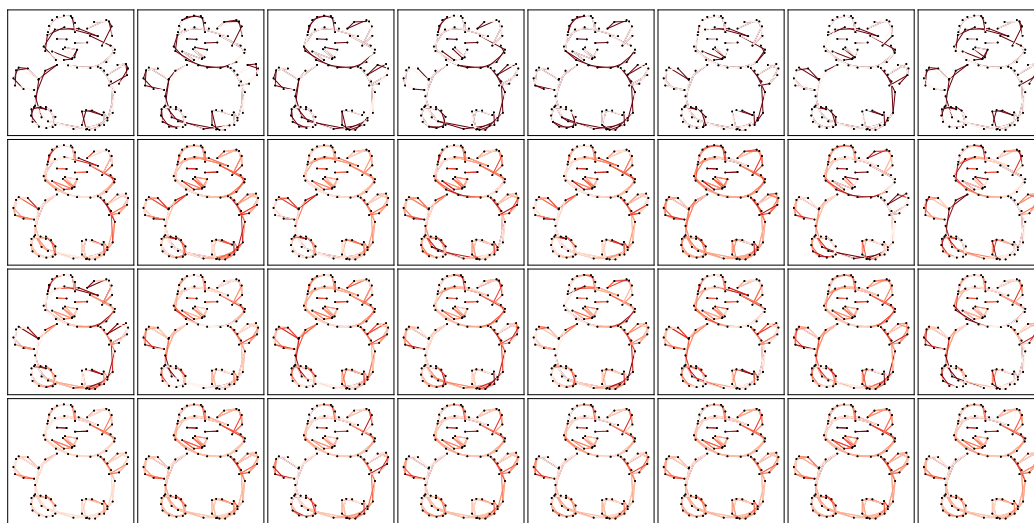
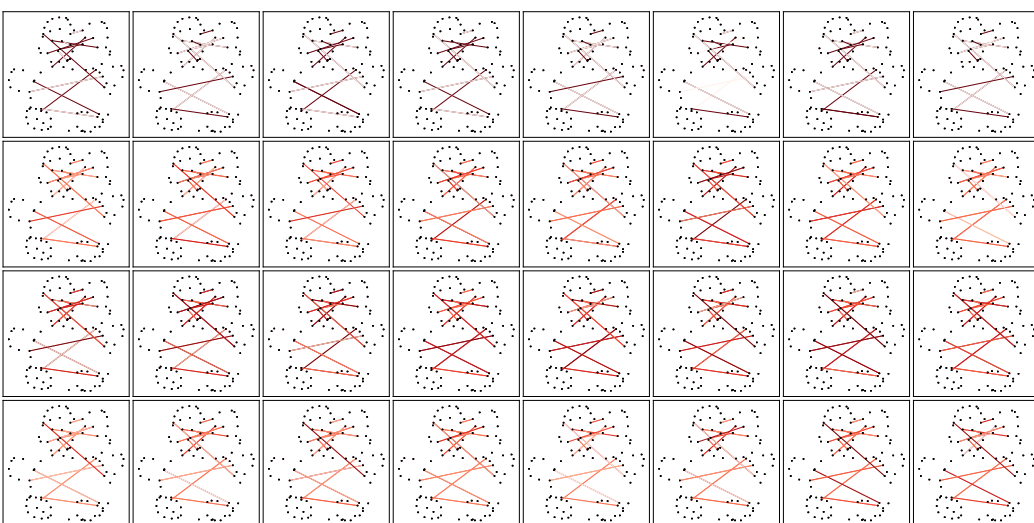
(a) $\mathbf{A}^{1\text{-hop}}$ (b) $\mathbf{A}^{2\text{-hop}}$ (c) $\mathbf{A}^{\text{global}}$

Fig. 7. Attention heads at each layer of MGT for a test set sample labelled *teddy*. Each layer has $I = 8$ attention heads per graph in total. Darker reds indicate higher attention values. Best viewed in color.

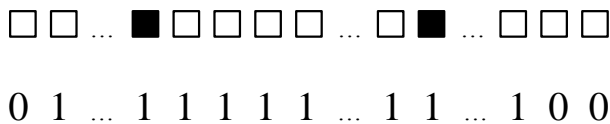


Fig. 8. A partially-connected graph illustration for a long sentence. The entities and the other words are denoted by the solid and hollow squares, respectively. The corresponding attention mask is also provided.

accuracy: ours (89.45%) vs. CNN [60] (86.60%). In particular, when we use Bidirectional Encoder Representations from Transformers (BERT) [63] as Transformer-based encoder, each sentence will be encoded as a fully-connected graph. Given a long sentence, if its two entities are overly far from each other, the RE model should give more attention on the words between and around the two entities. Therefore, we also use multiple graph structures to inject this domain-knowledge into the Transformer-based encoder: (i) Fully-connected: In the early and middle stages of training, we allow the transformer to encode each sentence as a fully-connected graph, regardless of its length. (ii) Partially-connected: In the last few epochs, if in a given long sentence its two entities are far apart, we force the transformer to encode the long sentence as a partially-connected graph, which consists of the words between and around the two entities. We use a binary attention mask to encode this. See Figure 8 for an illustration.

This experimental phenomenon further encourages us to explore the applications of using domain-specific graph structures to inject the domain-knowledge into Transformers in other modalities and tasks.

V. CONCLUSION

This paper introduces a novel representation of free-hand sketches as multiple sparsely connected graphs. We design a Multi-Graph Transformer (MGT) for capturing both geometric structure and temporal information from sketch graphs. The intrinsic traits of the MGT architecture include: (i) using graphs as universal representations of sketch geometry, as well as temporal and semantic information, (ii) injecting domain knowledge into Transformers through sketch-specific graphs, and (iii) making full use of multiple intra-stroke and extra-stroke graphs.

For sketch community: We, for the first time, propose to model sketches as sparsely connected graphs. For GNN community: We design a novel graph transformer model that considers prior/domain knowledge via multiple graph structures. This multi-graph modeling idea works well for both sketch and other modalities.

We hope MGT can serve as a foundation for future work in sketch applications and network architectures, motivating the community towards sketch representation learning using graphs. Additionally, for the graph neural network (GNN) community, we hope that MGT helps free-hand sketch become a new test-bed for GNNs.

VI. FUTURE WORK

Our future work will focus on applying our MGT as a general neural representation in various sketch tasks, e.g.,

sketch generation. More code and results will be updated continuously on our project page ⁸.

REFERENCES

- [1] D. Ha and D. Eck, "A neural representation of sketch drawings," *arXiv preprint arXiv:1704.03477*, 2017.
- [2] P. Xu, Y. Huang, T. Yuan, K. Pang, Y.-Z. Song, T. Xiang, T. M. Hospedales, Z. Ma, and J. Guo, "Sketchmate: Deep hashing for million-scale human sketch retrieval," in *Proceedings of the IEEE Conference on Computer Vision and Pattern Recognition*, 2018, pp. 8090–8098.
- [3] F. Liu, X. Deng, Y.-K. Lai, Y.-J. Liu, C. Ma, and H. Wang, "Sketchgan: Joint sketch completion and recognition with generative adversarial network," in *Proceedings of the IEEE Conference on Computer Vision and Pattern Recognition*, 2019, pp. 5830–5839.
- [4] R. K. Sarvadevabhatla, J. Kundu, and V. Babu R, "Enabling my robot to play pictonary: Recurrent neural networks for sketch recognition," in *Proceedings of the 24th ACM international conference on Multimedia*, 2016, pp. 247–251.
- [5] Y. Ye, Y. Lu, and H. Jiang, "Human's scene sketch understanding," in *Proceedings of the 2016 ACM on International Conference on Multimedia Retrieval*, 2016, pp. 355–358.
- [6] P. Sangkloy, N. Burnell, C. Ham, and J. Hays, "The sketchy database: learning to retrieve badly drawn bunnies," *ACM Transactions on Graphics*, vol. 35, no. 4, pp. 1–12, 2016.
- [7] L. Liu, F. Shen, Y. Shen, X. Liu, and L. Shao, "Deep sketch hashing: Fast free-hand sketch-based image retrieval," in *Proceedings of the IEEE conference on computer vision and pattern recognition*, 2017, pp. 2862–2871.
- [8] Y. Shen, L. Liu, F. Shen, and L. Shao, "Zero-shot sketch-image hashing," in *Proceedings of the IEEE Conference on Computer Vision and Pattern Recognition*, 2018, pp. 3598–3607.
- [9] J. Collomosse, T. Bui, and H. Jin, "Livesketch: Query perturbations for guided sketch-based visual search," in *Proceedings of the IEEE Conference on Computer Vision and Pattern Recognition*, 2019, pp. 2879–2887.
- [10] A. Dutta and Z. Akata, "Semantically tied paired cycle consistency for zero-shot sketch-based image retrieval," in *Proceedings of the IEEE Conference on Computer Vision and Pattern Recognition*, 2019, pp. 5089–5098.
- [11] S. Dey, P. Riba, A. Dutta, J. Lladós, and Y.-Z. Song, "Doodle to search: Practical zero-shot sketch-based image retrieval," in *Proceedings of the IEEE Conference on Computer Vision and Pattern Recognition*, 2019, pp. 2179–2188.
- [12] W. Chen and J. Hays, "Sketchygan: Towards diverse and realistic sketch to image synthesis," in *Proceedings of the IEEE Conference on Computer Vision and Pattern Recognition*, 2018, pp. 9416–9425.
- [13] Y. Lu, S. Wu, Y.-W. Tai, and C.-K. Tang, "Image generation from sketch constraint using contextual gan," in *Proceedings of the European Conference on Computer Vision*, 2018, pp. 205–220.
- [14] P. Xu, Z. Song, Q. Yin, Y. Song, and L. Wang, "Deep self-supervised representation learning for free-hand sketch," *IEEE Transactions on Circuits and Systems for Video Technology*, 2020.
- [15] H. Lin, Y. Fu, X. Xue, and Y.-G. Jiang, "Sketch-bert: Learning sketch bidirectional encoder representation from transformers by self-supervised learning of sketch gestalt," in *Proceedings of the IEEE Conference on Computer Vision and Pattern Recognition*, 2020, pp. 6758–6767.
- [16] Q. Yu, Y. Yang, Y.-Z. Song, T. Xiang, and T. Hospedales, "Sketch-a-net that beats humans," *arXiv preprint arXiv:1501.07873*, 2015.
- [17] A. Vaswani, N. Shazeer, N. Parmar, J. Uszkoreit, L. Jones, A. N. Gomez, Ł. Kaiser, and I. Polosukhin, "Attention is all you need," *Advances in neural information processing systems*, vol. 30, pp. 5998–6008, 2017.
- [18] P. W. Battaglia, J. B. Hamrick, V. Bapst, A. Sanchez-Gonzalez, V. Zambaldi, M. Malinowski, A. Tacchetti, D. Raposo, A. Santoro, R. Faulkner et al., "Relational inductive biases, deep learning, and graph networks," *arXiv preprint arXiv:1806.01261*, 2018.
- [19] K. Li, K. Pang, Y.-Z. Song, T. Xiang, T. M. Hospedales, and H. Zhang, "Toward deep universal sketch perceptual grouper," *IEEE Transactions on Image Processing*, vol. 28, no. 7, pp. 3219–3231, 2019.
- [20] P. Xu, "Deep learning for free-hand sketch: A survey," *arXiv preprint arXiv:2001.02600*, 2020.

⁸https://github.com/PengBoXiangShang/multigraph_transformer

- [21] A. Krizhevsky, I. Sutskever, and G. E. Hinton, "Imagenet classification with deep convolutional neural networks," *Communications of the ACM*, vol. 60, no. 6, pp. 84–90, 2017.
- [22] J. Song, Q. Yu, Y.-Z. Song, T. Xiang, and T. M. Hospedales, "Deep spatial-semantic attention for fine-grained sketch-based image retrieval," in *Proceedings of the IEEE International Conference on Computer Vision*, 2017, pp. 5551–5560.
- [23] Q. Jia, M. Yu, X. Fan, and H. Li, "Sequential dual deep learning with shape and texture features for sketch recognition," *arXiv preprint arXiv:1708.02716*, 2017.
- [24] L. Li, C. Zou, Y. Zheng, Q. Su, H. Fu, and C. L. Tai, "Sketch-r2cnn: An rnn-rasterization-cnn architecture for vector sketch recognition," *IEEE Transactions on Visualization and Computer Graphics*, 2020.
- [25] Z. Wu, S. Pan, F. Chen, G. Long, C. Zhang, and S. Y. Philip, "A comprehensive survey on graph neural networks," *IEEE Transactions on Neural Networks and Learning Systems*, pp. 1–21, 2020.
- [26] J. Bruna, W. Zaremba, A. Szlam, and Y. Lecun, "Spectral networks and locally connected networks on graphs," in *International Conference on Learning Representations*, 2014.
- [27] M. Defferrard, X. Bresson, and P. Vandergheynst, "Convolutional neural networks on graphs with fast localized spectral filtering," *Advances in neural information processing systems*, vol. 29, pp. 3844–3852, 2016.
- [28] S. Sukhbaatar, R. Fergus *et al.*, "Learning multiagent communication with backpropagation," *Advances in neural information processing systems*, vol. 29, pp. 2244–2252, 2016.
- [29] T. N. Kipf and M. Welling, "Semi-supervised classification with graph convolutional networks," in *International Conference on Learning Representations*, 2017.
- [30] W. Hamilton, Z. Ying, and J. Leskovec, "Inductive representation learning on large graphs," in *Advances in neural information processing systems*, 2017, pp. 1024–1034.
- [31] F. Monti, D. Boscaini, J. Masci, E. Rodola, J. Svoboda, and M. M. Bronstein, "Geometric deep learning on graphs and manifolds using mixture model cnns," in *Proceedings of the IEEE Conference on Computer Vision and Pattern Recognition*, 2017, pp. 5115–5124.
- [32] U. S. Shanthamallu, J. J. Thiagarajan, H. Song, and A. Spanias, "Gramme: Semisupervised learning using multilayered graph attention models," *IEEE Transactions on Neural Networks and Learning Systems*, vol. 31, no. 10, pp. 3977–3988, 2020.
- [33] S. Edunov, M. Ott, M. Auli, and D. Grangier, "Understanding back-translation at scale," *arXiv preprint arXiv:1808.09381*, 2018.
- [34] Q. Wang, B. Li, T. Xiao, J. Zhu, C. Li, D. F. Wong, and L. S. Chao, "Learning deep transformer models for machine translation," *arXiv preprint arXiv:1906.01787*, 2019.
- [35] A. Radford, K. Narasimhan, T. Salimans, and I. Sutskever, "Improving language understanding by generative pre-training," *OpenAI Blog*, 2018.
- [36] Z. Dai, Z. Yang, Y. Yang, W. W. Cohen, J. Carbonell, Q. V. Le, and R. Salakhutdinov, "Transformer-xl: Attentive language models beyond a fixed-length context," *arXiv preprint arXiv:1901.02860*, 2019.
- [37] J. Devlin, M.-W. Chang, K. Lee, and K. Toutanova, "Bert: Pre-training of deep bidirectional transformers for language understanding," *arXiv preprint arXiv:1810.04805*, 2018.
- [38] Z. Yang, Z. Dai, Y. Yang, J. Carbonell, R. Salakhutdinov, and Q. V. Le, "Xlnet: Generalized autoregressive pretraining for language understanding," *arXiv preprint arXiv:1906.08237*, 2019.
- [39] D. Bahdanau, K. Cho, and Y. Bengio, "Neural machine translation by jointly learning to align and translate," *arXiv preprint arXiv:1409.0473*, 2014.
- [40] P. Veličković, G. Cucurull, A. Casanova, A. Romero, P. Liò, and Y. Bengio, "Graph Attention Networks," in *International Conference on Learning Representations*, 2018.
- [41] Z. Ye, Q. Guo, Q. Gan, X. Qiu, and Z. Zhang, "Bp-transformer: Modelling long-range context via binary partitioning," *arXiv preprint arXiv:1911.04070*, 2019.
- [42] N. Srivastava, G. Hinton, A. Krizhevsky, I. Sutskever, and R. Salakhutdinov, "Dropout: A simple way to prevent neural networks from overfitting," *The journal of machine learning research*, vol. 15, no. 1, pp. 1929–1958, 2014.
- [43] K. He, X. Zhang, S. Ren, and J. Sun, "Deep residual learning for image recognition," in *Proceedings of the IEEE conference on computer vision and pattern recognition*, 2016, pp. 770–778.
- [44] S. Ioffe and C. Szegedy, "Batch normalization: Accelerating deep network training by reducing internal covariate shift," *arXiv preprint arXiv:1502.03167*, 2015.
- [45] M. Eitz, J. Hays, and M. Alexa, "How do humans sketch objects?" *ACM Transactions on graphics*, vol. 31, no. 4, pp. 1–10, 2012.
- [46] A. Paszke, S. Gross, F. Massa, A. Lerer, J. Bradbury, G. Chanan, T. Killeen, Z. Lin, N. Gimelshein, L. Antiga *et al.*, "Pytorch: An imperative style, high-performance deep learning library," in *Advances in neural information processing systems*, 2019, pp. 8026–8037.
- [47] X. Glorot, A. Bordes, and Y. Bengio, "Deep sparse rectifier neural networks," in *Proceedings of the fourteenth international conference on artificial intelligence and statistics*, 2011, pp. 315–323.
- [48] D. P. Kingma and J. Ba, "Adam: A method for stochastic optimization," *arXiv preprint arXiv:1412.6980*, 2014.
- [49] S. Hochreiter and J. Schmidhuber, "Long short-term memory," *Neural computation*, 1997.
- [50] K. Cho, B. Van Merriënboer, D. Bahdanau, and Y. Bengio, "On the properties of neural machine translation: Encoder-decoder approaches," *arXiv preprint arXiv:1409.1259*, 2014.
- [51] C. Szegedy, V. Vanhoucke, S. Ioffe, J. Shlens, and Z. Wojna, "Rethinking the inception architecture for computer vision," in *Proceedings of the IEEE conference on computer vision and pattern recognition*, 2016, pp. 2818–2826.
- [52] M. Sandler, A. Howard, M. Zhu, A. Zhmoginov, and L.-C. Chen, "Mobilenetv2: Inverted residuals and linear bottlenecks," in *Proceedings of the IEEE conference on computer vision and pattern recognition*, 2018, pp. 4510–4520.
- [53] G. Huang, Z. Liu, L. Van Der Maaten, and K. Q. Weinberger, "Densely connected convolutional networks," in *Proceedings of the IEEE conference on computer vision and pattern recognition*, 2017, pp. 4700–4708.
- [54] X. Bresson and T. Laurent, "An experimental study of neural networks for variable graphs," in *International Conference on Learning Representations Workshop*, 2018.
- [55] K. Simonyan and A. Zisserman, "Very deep convolutional networks for large-scale image recognition," *arXiv preprint arXiv:1409.1556*, 2014.
- [56] J.-J. Liu, Q. Hou, M.-M. Cheng, C. Wang, and J. Feng, "Improving convolutional networks with self-calibrated convolutions," in *Proceedings of the IEEE Conference on Computer Vision and Pattern Recognition*, 2020, pp. 10096–10105.
- [57] D. Haase and M. Amthor, "Rethinking depthwise separable convolutions: How intra-kernel correlations lead to improved mobilenets," in *Proceedings of the IEEE Conference on Computer Vision and Pattern Recognition*, 2020, pp. 14600–14609.
- [58] R. Pascanu, T. Mikolov, and Y. Bengio, "On the difficulty of training recurrent neural networks," in *International conference on machine learning*, 2013, pp. 1310–1318.
- [59] M. Shoenybi, M. Patwary, R. Puri, P. LeGresley, J. Casper, and B. Catanzaro, "Megatron-lm: Training multi-billion parameter language models using gpu model parallelism," *arXiv preprint arXiv:1909.08053*, 2019.
- [60] X. Guo, H. Zhang, H. Yang, L. Xu, and Z. Ye, "A single attention-based combination of cnn and rnn for relation classification," *IEEE Access*, vol. 7, pp. 12467–12475, 2019.
- [61] H. Wang, M. Tan, M. Yu, S. Chang, D. Wang, K. Xu, X. Guo, and S. Potdar, "Extracting multiple-relations in one-pass with pre-trained transformers," *arXiv preprint arXiv:1902.01030*, 2019.
- [62] I. Hendrickx, S. N. Kim, Z. Kozareva, P. Nakov, D. O. Séaghdha, S. Padó, M. Pennacchiotti, L. Romano, and S. Szpakowicz, "Semeval-2010 task 8: Multi-way classification of semantic relations between pairs of nominals," *arXiv preprint arXiv:1911.10422*, 2019.
- [63] J. Devlin, M.-W. Chang, K. Lee, and K. Toutanova, "Bert: Pre-training of deep bidirectional transformers for language understanding," *arXiv preprint arXiv:1810.04805*, 2018.